Wiper Systems with Flexible Structures - Instabilities Analysis and Correlation with a Theoretical Model

Carine Chevennement-Roux, Régis Grenouillat, Thomas Dreher, Patrick Alliot, Evelyne Aubry, Jean-Pierre Lainé, Louis Jézéquel

Wiper Systems With Flexible Structures – Instabilities Analysis and Correlation with a Theoretical Model

Carine Chevennement-Roux, Régis Grenouillat and Thomas Dreher
Valeo Wiper Systems

Patrick Alliot and Evelyne Aubry
ESSAIM

Jean-Pierre Lainé and Louis Jézéquel
ECL

ABSTRACT

Optimizing the wiper system performance motivates the design engineer to create a product as robust as possible against the occurrence of wipe defects related to vibratory phenomena between the rubber blade and the windshield. In some configurations, these vibrations generate visual or audible annoyance for the driver. These instabilities phenomena only appear under specific operating and environmental conditions characterized by windshield moisture and cleanness, contact pressure of the rubber blade on the glass, attack angle of the wiper blade on the windshield, component stiffness, windshield curvature etc. In the process of eliminating all potential instabilities, modeling the wiper system structures can contribute to understand its working dynamics. Therefore, a new computation tool is developed and validated by experimentation on a specific test bench.

INTRODUCTION

Windshield wiper systems of modern vehicles are more and more complex and must answer increasingly severe specifications and requirements of security. Recently, a particular effort was made to ensure a constant contact force of the rubber on the entire glass surface covered by wipe pattern. In the same time, increasingly complex shapes of windshields are developed. This significant condition was subject of previous studies on the rubber glass interface [1], [2] and optimization of the windshield shape [3]. Moreover, the optimization of a wiper system, which is an essential objective for an equipment supplier such as Valeo Wiper Systems, leads the design engineer to seek to eliminate all possible wiping defects. Part of these defects is caused by the appearance of dynamic vibratory phenomena between the rubber blade and the windshield.

In this field, the research of the Valeo Wiper Systems engineers is focused on an elaborate knowledge of the wiper system dynamics and on the various parameters influencing the system instabilities. The contribution of this study is to add a new model to the existing set of computation software that is currently used for product design. Based on this tool, the designers will be able to adopt the optimum set of parameters for a robust wiper system.

At the beginning of the study on wiper systems, we sought the analogy with other mechanical systems involving friction, such as the clutches and brakes. While there is few documentation on wiper systems instabilities, engineers of clutches and brakes already have an important know-how on instabilities on their applications. In particular, models on stick-slip and sprag-slip phenomena have been developed and validated [4], [5]. Some of these concepts are appropriated to be applied in the wiper systems field.

SYSTEM DESCRIPTION

A conventional wiper system (Figure 1) comprises an electric motor and a linkage mechanism which converts the rotational movement of the motor into the back and forth motions of the wiper arms [6]. The mechanical structure of the wiper blades, which is attached to the arm tips, holds the rubber blade which drains the water off the windshield [7] and [2].

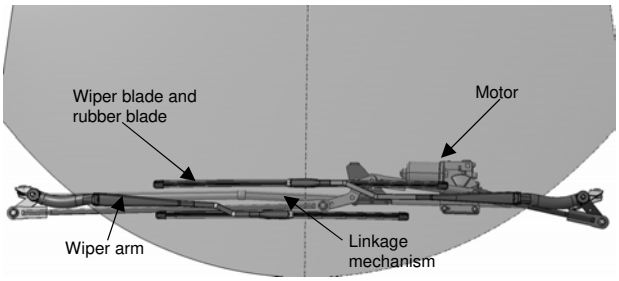

Figure 1: Wiper system on a windshield description

Various parameters have a significant influence on the occurrence of wipe defects. There are three main categories of parameters: firstly, system parameters (wiper blade inertia and dimensions, stiffness, twist angles, contact pressure, geometry of the windshield …), secondly, surface and material characteristics (roughness, friction on the rubber-glass contact, Young modulus…) and finally, environmental and operating parameters (temperature, humidity, cleanness…).

In our study, we only focus on main parameters influencing the dynamic behavior of the system. One of the most critical parameter for the wipe quality is the attack angle which is defined as the angle between the wiper blade symmetry plane and the vector normal to the outer glass surface (Figure 2).

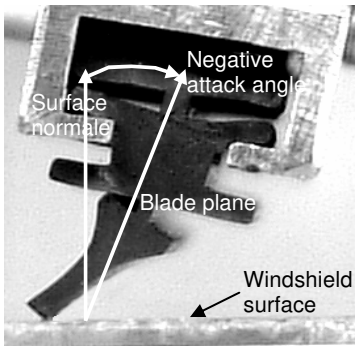

Figure 2: Attack angle definition

Moreover, the windshield moisture and cleanness and the characteristics of the rubber blade influence the wiping condition. These properties are taken into account by the variation of the friction coefficient [8].

Lastly, another critical parameter is the arm tip force applied on the blade. In order to obtain a uniform contact force (expressed in N/m) under the rubber blade, it can be adjusted by a steel spring.

EXPERIMENTAL ANALYSIS

TEST RIG

We carry out our experimental tests on a flat glass with a specific wiper system and a wiper motor which ensures a continuous rotating movement. Such an experimental rig allows to eliminate the transient phenomena and presents the advantages to be more stable with a higher accuracy and robustness.

The aim of the measurements is a parametric study with two main parameters: the tip force applied at the hook point and the attack angle under various conditions of wet glass, dry glass or drying glass. We carry out experiments with a flexible wiper system: the Valeo Flat Blade.

Accelerometers are placed on several locations on the wiper arm and blade, in order to quantify the vibratory level and to identify the instability frequencies. Using several accelerometers at the same time enables to determine the mode shape of the vibration. Particular care is taken on the fact that the mass of the accelerometers may influence the inertia of the components and so the instability frequencies.

The Figure 3 and Figure 4 show the test rig and the accelerometers location on the wiper system to be tested. Accelerometers are located to measure displacements in the Z direction (perpendicular to the glass) and in the Y direction (wiper blade displacement direction) (Figure 3).

Figure 3: Experimental rig

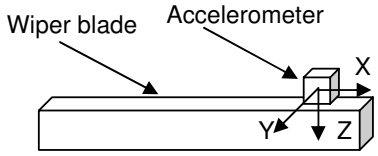

Figure 4: Schematic view of the blade with an accelerometer representing the coordinate system

RESULTS AND OBSERVATIONS

Time acceleration signals are processed to obtain frequency spectra when instabilities appear or not. It is important to observe also the frequency peaks to detect occurrence of flutter instabilities.

Some examples of amplitude spectra obtained are shown below (Figure 5 and Figure 6).

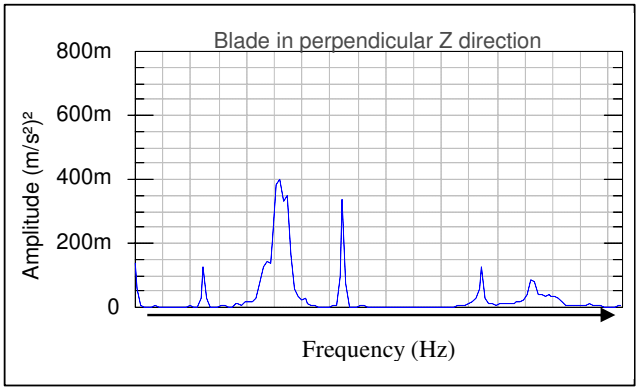

Figure 5: Amplitude curves without instabilities

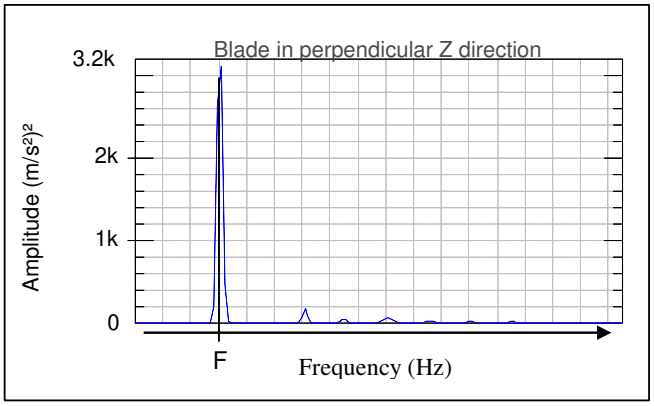

Figure 6 : Amplitude curves with instabilities

The Figure 5 presents results without instabilities where the eigen frequencies of the structure can be identified. These eigen frequencies are low frequencies and can be overlapped with electromagnetic and vibratory background noises. The system structural modes can vary due to the friction coefficient coupling. The occurrence of chatter destabilizes these eigen frequencies, so then there is a coupling of the eigen mode. This instable frequency is noted F.

Then comparing these two figures, when instabilities appear, the level of the spectra amplitude is at least 100 times higher than the level when the system is stable. Moreover, when chatter appears, the system has a vertical displacement amplitude of 0.4 millimeter.

The post-processing of all the results shows a variation of the amplitude spectra along the blade.

Generally, the instabilities level of the amplitude spectra is higher for a tacky glass than for a wet glass. Moreover, the instabilities level can vary according to the nominal pressure applied to the system.

The study of the experimental results shows a coupling between the friction phenomena and the structural mode. This coupling creates structural instabilities with the frequency F.

FRICTION COEFFICIENT INFLUENCE

Friction between the rubber lip and the glass surface depends on the humidity. The mean friction coefficient is measured through the total resistive torque on the wiper shaft. For each test configuration (applied pressure, attack angle) the mean friction coefficient is determined from the ration between normal and tangent force.

These tests have been carried out varying pressure and attack angle. The Table 1 and Table 2 show examples obtained for two attack angles and three pressures.

Friction coefficient Parameters	0,2 – 0,4	>1
7° et 13 N/m	Stable	Stable
7° et 15 N/m	Stable	Stable
7° et 18 N/m	Stable	Stable

Table 1

Friction coefficient Parameters	0,2 – 0,4	>1
15° et 13 N/m	Stable	Stable
15° et 15 N/m	Stable	Instable
15° et 18 N/m	Stable	Instable

Table 2

In wet glass condition, the friction coefficient varies from 0,2 to 0,4.

In dry glass condition, the friction coefficient varies from 0,8 to 0,1.

In tacky glass condition, the friction coefficient is higher than 1.

THEORETICAL MODEL - MODELING

The computational modeling is based on the Finite Elements Model of the arm and blade system. The wiper system is divided in three distinct sub-systems which are the arm, the wiper blade and then the rubber blade.

The dynamics of each sub-system is represented by a certain number of eigenmodes. The number of modes to be taken into account for the system is determined by the frequency range that is of interest.

The Figure 7 shows the wiping system in the chosen coordinate systems R (O; X, Y, Z).

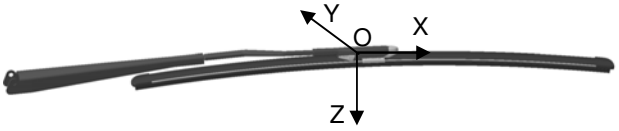

Figure 7: Wiper system in the reference mark of space R (O; X, Y, Z)

ARM MODELING

First, we perform a static calculation on the arm model to obtain the arm geometry for different attack angles.

Then, from the Finite Element Model of the arm, we perform a Guyan Condensation [9] in order to extract 30 master degrees of freedom (dof). This reduced model is validated by comparison with a full FEM model for modal calculation. Among these 30 dof, 3 dof represent the link between the arm and the spring and 6 dof represent the link between the arm and the wiper blade.

The resulting mass and stiffness matrices are assembled with the stiffness term of the spring. A second dof reduction is obtained through a Craig and Bampton sub-structuration method [9], [10]. This way, we can reduce the number of dof down to 8 dof of which 6 represent the link arm-blade and 2 eigen dynamic modes (first vertical and horizontal bending modes of the arm).

Finally, the arm is modeled by an 8x8 mass and stiffness matrices.

WIPER BLADE MODELING

A first study has already been undertaken with a rigid wiper blade [11]. Here, we consider a flexible wiper blade.

The wiper blade deformations for bending directions are taken into account through a Rayleigh-Ritz procedure:

$\phi = \lambda \frac{x^2}{(l/2)^2}$ with ϕ a trial function, λ the generalized displacement and l is the length of the wiper blade.

In order to calculate the mass matrix of the flexible wiper blade, we calculate its kinetic energy in its gravity center.

The kinetic energy is written as below :

$$Ec = \frac{1}{2}\int_{-l/2}^{l/2} (\rho dx)(\dot{u}_X^2 + \dot{u}_Y^2 + \dot{u}_Z^2) \qquad \text{(Equ. 1)}$$

with ρ is the mass per unit length and ux, uy and uz are the gravity center displacements written as (Equ. 2).

$$\vec{u}_G = \vec{U}_o + \vec{\theta} \wedge \vec{OG} = \begin{pmatrix} U_X \\ U_Y \\ U_Z \end{pmatrix} + \begin{pmatrix} \theta_X \\ \theta_Y \\ \theta_Z \end{pmatrix} \wedge \begin{pmatrix} x \\ aa \\ bb \end{pmatrix} + \begin{pmatrix} 0 \\ \phi_{Y1} \ldots \phi_{Y2} \\ \phi_{Z1} \ldots \phi_{Z2} \end{pmatrix}$$

(Equ. 2)

with aa and bb, the gravity center coordinates in R.

U_X, U_Y and U_Z are the translation displacements and θ_X, θ_Y, θ_Z, are the rotation angle of the hook point.

Substituting (Equ.2) in (Equ.1), we obtain:

$$Ec = \frac{1}{2}\dot{q}^T [Md] \dot{q} \qquad \text{(Equ. 3)}$$

with Md is the mass matrix of the flexible wiper blade and q^T the generalized vector displacement:

$$q^T = [U_X\ U_Y\ U_Z\ \theta_X\ \theta_Y\ \theta_Z\ \lambda_{Y1}\ \lambda_{Z1} \cdots \lambda_{Y4}\ \lambda_{Z4}]$$

Then, the stiffness matrix associated with the wiper blade deformability is calculated. The matrix depends on the Young modulus E and on the inertia I of the wiper blade. The parameters EI are updated on the results of the modal analysis of the wiper blade.

The potential energy is written as below:

$$Ep = \frac{1}{2}\int_{-l/2}^{l/2} EI(\ddot{\phi}_y(x))^2 + EI(\ddot{\phi}_z(x))^2 dx \qquad \text{(Equ. 4)}$$

So we obtain

$$Ep = \frac{1}{2} q^T [Kd] q \qquad \text{(Equ. 5)}$$

Kd is the stiffness matrix of the flexible wiper blade.

The arm and the wiper blade are assembled coupling the terms in their mass and stiffness matrices. This coupling is represented by a pivot connection around Y axis between the arm and the wiper blade. This pivot connection brings an additional dof to the matrix system.

The mass and the stiffness matrices for the arm-wiper blade system have a rank of 9 plus the dof representing the deformations of the wiper blade. To this system, we add the deformation energy of the rubber blade to the deformation energy of the arm-wiper blade system.

RUBBER BLADE MODELING

Deformation model

The rubber blade model is a non linear model, taking into account hyper elastic material behavior, glass-rubber contact and rubber auto-contacts. We set different hypothesis.

- inertia forces associated with the rubber lip deformations are neglected;
- longitudinal coupling of the rubber blade is neglected;
- consider a normal force F_N applied to the system and a friction force according to the Coulomb law $f = \mu F_N$ where μ is the dynamic friction [12] and [13].

Quasi-static study will take into account these three hypothesis.

First step: we perform a quasi-static study of the rubber blade from its Finite Element model in order to prove the existence of stable static solutions.

Quasi-static equilibrium position: the normal force F_N due to the arm spring, crushes the rubber blade against the glass. Three solutions are possible to obtain the quasi-static stable solutions (Figure 8):

- solution 1 in the wiping sense;
- solution 2 in compression;
- solution 3 non reversal position of blade.

To ensure stability of the non linear solution (multiple solutions), quasi-static calculations are carried out controlling the vertical force applied on the rubber blade and the horizontal displacement of the contact point rubber blade-glass.

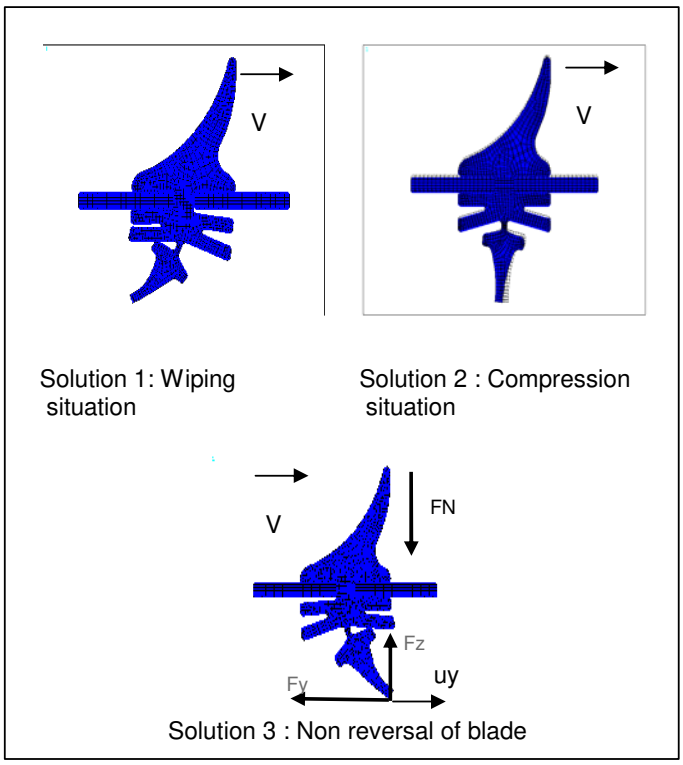

Figure 8: Rubber blade position

Out of those three solutions, a choice is made according to operating condition:

- solutions 1 correspond to a wiping situation with V>0;
- solutions 2 with μ>0, either correspond to a wiping situation when V>0 for uy>0, or to a non reversal situation when V>0 for uy>0;
- solutions 3 with μ>0 correspond to a non reversal of blade with V>0.

From these simulation results and for various vertical force values applied on the rubber blade and the friction coefficient, we can calculate:

- horizontal displacement of the contact point related to the wiper blade : uy;
- vertical displacement of the wiper blade related to the glass: uz;
- tangent vertical stiffness defined from the derived $k = \frac{dF_N}{duy}$ for a constant μ around the equilibrium position by a bi-linear interpolation.

The results of the quasi-static calculation give the horizontal displacement uy and the vertical displacement uz. These displacements are the difference between the

reference position and the initial position. The reference position is defined as: rubber blade is not deformed and is in contact with the glass.

From uy and uz, we calculate the value of the parameters a and b (Figure 9) such as $a = a_0 + uy$ where a_0 corresponds to the horizontal distance between the contact point of the rubber blade none deformed with the glass and the hook point and uy is the displacement horizontal of the contact point compared to this reference position a_0. In the same way, we obtain $b = b_0 + uz$ is the vertical displacement.

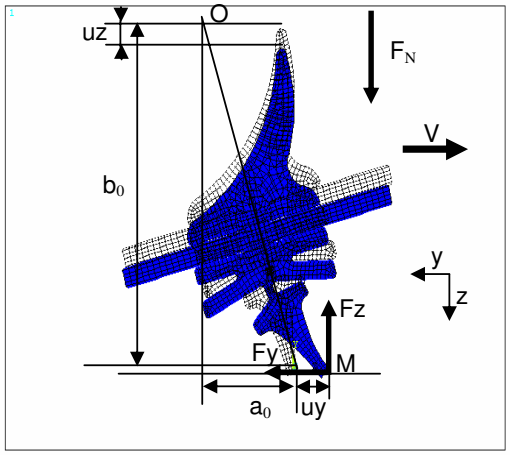

Figure 9 : Definition of a and b

The tangent stiffness k is calculated by a bi-linear interpolation of the quasi-static simulation results. Indeed, in order to obtain better accuracy for the k calculation, we perform a first interpolation with the applied force and then a second interpolation with the friction coefficient.

For each kind of solution, we have quasi-static solutions potentially stable and quasi-static solutions potentially unstable (negative stiffness) according to the sign of k.

Thus, for the solutions 1, we have k>0 indicating quasi-static stable solutions; we obtain the same result for solutions 3. However, for solutions 2, k can be negative or positive, so we can obtain stable or instable quasi-static solutions.

The parameters a, b and k are characteristics of the rubber blade and represent the input parameters for the dynamic study.

Rubber blade model

Once local tangent stiffness k obtained, we calculate the stiffness matrix of the rubber blade.

We consider small displacements around the quasi-static equilibrium position. This position depends on the spring stiffness, the friction coefficient and the rubber blade stiffness. Thus, for small displacements, the generalized effort vector F of the glass on the rubber blade will depend linearly on the generalized displacement vector q of the wiper blade through the friction coefficient, the deformability and the static deformation of the rubber blade. Finally, we obtain the linearised stiffness matrix which depends on the friction coefficient and the geometry of the static deformation of the rubber blade.

So we obtain the stiffness matrix of the rubber blade Kdl calculated at the link point between the arm and the wiper blade.

This stiffness matrix of the rubber blade can be written as below:

$$F = [Kdl]q \qquad \text{(Equ. 6)}$$

with Kdl the stiffness matrix of the rubber blade.

The generalized effort vector is

$$F^T = [F_X\ F_Y\ F_Z\ M_X M_Y\ M_Z\ F_{dY1}\ F_{dZ1} \cdots F_{dY4}\ F_{dZ4}]$$

with F the forces and M the torques

and the generalized displacement vector

$$q^T = [U_X\ U_Y\ U_Z\ \theta_X\ \theta_Y\ \theta_Z\ \lambda_{Y1}\ \lambda_{Z1} \cdots \lambda_{Y4}\ \lambda_{Z4}]$$

Displacements are expressed at the link point between the arm and the wiper blade:

$$\vec{u}_M = \vec{U}_o + \vec{\theta} \wedge \vec{OM} = \begin{pmatrix} U_X \\ U_Y \\ U_Z \end{pmatrix} + \begin{pmatrix} \theta_X \\ \theta_Y \\ \theta_Z \end{pmatrix} \wedge \begin{pmatrix} x \\ a \\ b \end{pmatrix} + \begin{pmatrix} 0 \\ \phi_Y \\ \phi_Z \end{pmatrix} \qquad \text{(Equ. 7)}$$

a and b are the link point coordinates.

FLUTTER INSTABILITIES STUDY

INSTABILITY AREA

Once calculated the mass and stiffness matrices corresponding to the arm and blade system, we obtain the equation system below:

$$[MF]\left[\ddot{Q}\right] + [KF][Q] = 0 \qquad \text{(Equ. 8)}$$

with [MF] is the final mass matrix,

[KF] the final stiffness matrix, which is non symmetric due to friction coupling terms,

Q is the generalized vector such as:

$$Q^T = [d1\ d2\ U_X\ U_Y\ U_Z\ \theta_X\ \theta_{Yar}\ \theta_Z\ \theta_{Ywb}\ \lambda_Y\ \lambda_Z]$$

(Equ. 9)

with d1 and d2 represent the two first dynamic eigen modes of the arm. Moreover, θ_{Yar} is the arm rotation and θ_{Ywb} is the blade rotation around Y axis at the hook point.

Dynamic stability is tested in the neighborhood of each realistic equilibrium point.

According to the set of input parameters (arm force, friction coefficient and various attack angles) we calculate eigenvectors and eigenvalues of the equation system (Equ. 8) in order to detect flutter instabilities regions (i.e. eigenvalues with positive real part and non null imaginary part) [14].

Instability areas for the solution 1 with an attack angle of 15° are examined in Figure 10 in function of (F, μ).

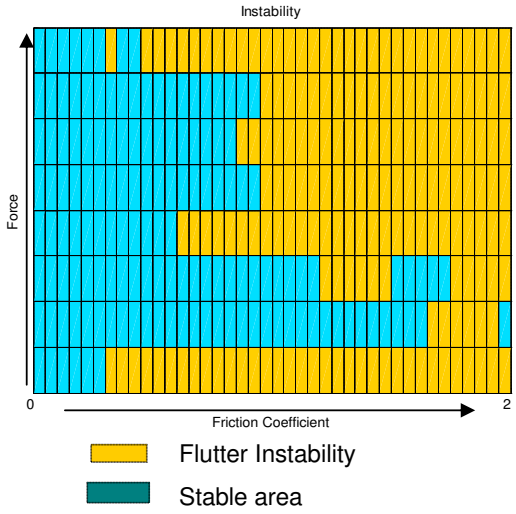

Figure 10: Instability areas for solutions 1 for an attack angle of 15°

EIGENVALUE EVOLUTION

The root locus in Figure 11 gives the eigenmode evolution.

The wiper system stability is tested by studying of the eigenvalue evolution versus the friction coefficient μ for given attack angle and force arm. We are interested in the real part and the imaginary part of the solution of the equation system (Equ. 8).

An example with an attack angle of 15°, an arm force of 15 N/m considering a friction coefficient μ from 0 to 2 is showed (Figure 11, Figure 12 and Figure 13).

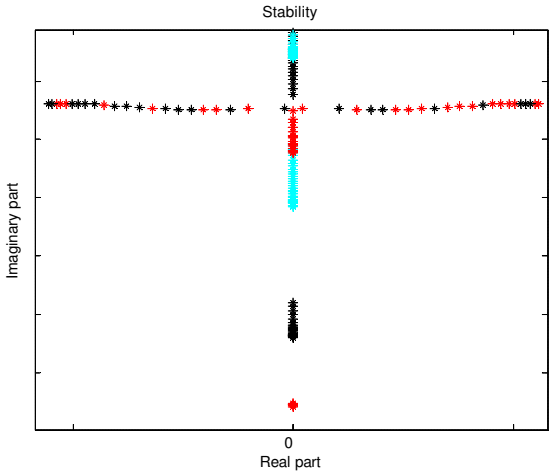

Figure 11: Root locus

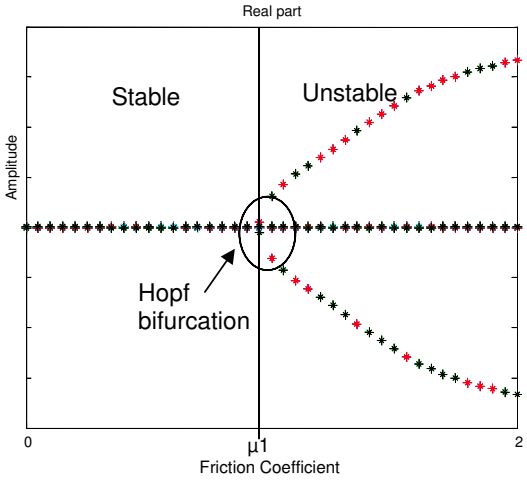

Figure 12: Real part of the system - F = 15 N/m, attack angle = 15°

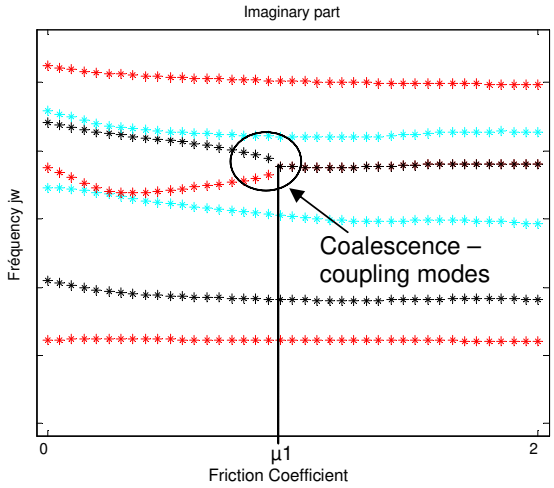

Figure 13: Imaginary part of the system - F = 15 N/m, attack angle = 15°

On the figure 12, we observe two different areas:

- 1st area : μ<μ1 : stable area (eigenvalue with null real part);
- 2nd area : μ>μ1 : instable area (eigenvalue with positive real part and non null imaginary part), flutter instability with a Hopf bifurcation at μ=μ1 with a point of coalescence of two modes [15], [16].

So in this case, the coupling mode creates the flutter instability for μ>μ1 with the frequency F.

EIGENVECTOR EVOLUTION

Generally, system eigenmodes appear separately. However, when friction is involved, it may happen that two eigenvalues are combined as one single system mode. In this case, this combined eigenmode creates instabilities. In our study, we observe combination of mode 4 and 5 when μ>μ1. This causes the instability of frequency F.

When this instability occurs, the displacement of the system is characterized by the corresponding eigenvector. This modal shape can be described in terms of system state variables or in terms of modal displacement (Figure 14).

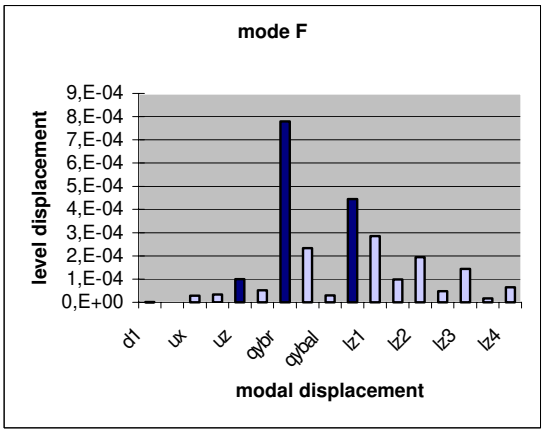

Figure 14: Modal displacement

Such a graph allows to understand the phenomena and to deduct the displacement of the system; but it does not give information on the instability amplitude.

THEORETICAL MODEL VALIDATION

The theoretical model is validated in three steps:

- Comparison of calculated eigen modes with results from experimental modal analysis of each component;
- In some cases, it was necessary to calibrate an individual mode. This is mainly due to the fact that some physical aspects are difficult to be taken into account (plays);
- Final validation is obtained by comparison of the instability chart (Figure 15) with experimental observation of instabilities on the 360° test bench.

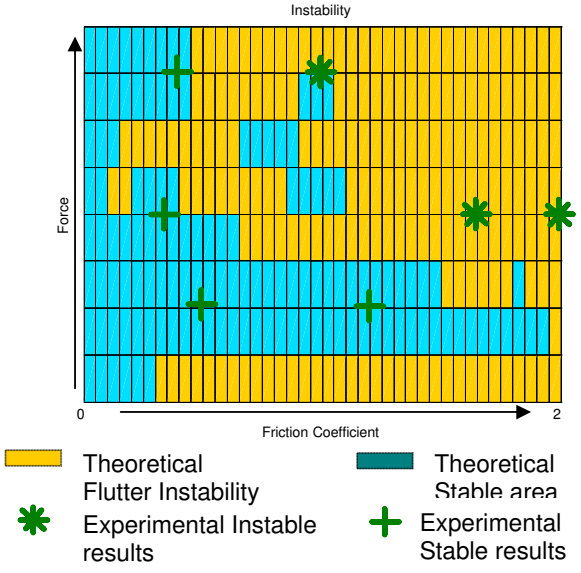

Figure 15: Instability areas of the system for wiping solutions 1 with an attack angle of 15° with added mass

Unlike the input parameter Force fixed, the friction coefficient is a measurement result, so the experimental results cannot reproduce the entire range of the friction coefficient.

SENSITIVITY ANALYSIS

A sensitivity analysis is performed in order to show the high sensitivity to the system of the parameters. Indeed, the instable area varies according to the parameter modified. Such analysis can be performed with the mass, the stiffness, the dimensions or the damping of the system.

The graph in Figure 16 is calculated without small mass added along the wiper blade. The comparisons between Figure 15 and Figure 16 shows that mass added introduce little flutter instabilities at low divergence for medium force.

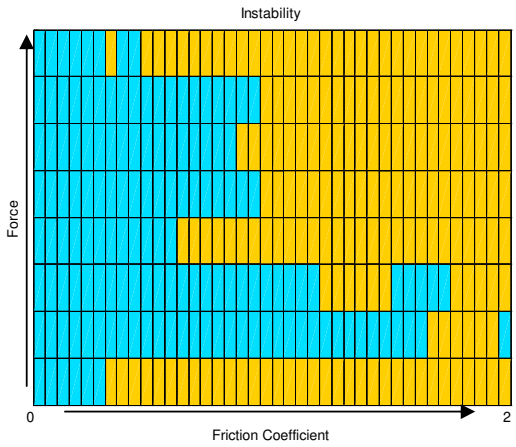

Figure 16: Instability areas of the system for wiping solutions 1with an attack angle of 15° without added mass

As the theoretical model is validated, it can be used as a tool to predict the instabilities tendency (such as chatter or judder) according to design parameters of the system. For example, we can vary the structural parameters of the wiper system in order to obtain the new area of stability. So a stability study with such a model will allow us to obtain a new system as robust as possible. Finally, this theoretical model will help the designer to obtain design rules and new design ideas.

CONCLUSION

The experimental tests provide a quantitative characterization of the system. The stable and instable areas for the most influent parameters emerge from this study. The experimental results give us information on the frequency, the amplitude and the shape of the instabilities.

A new computer model of wiper systems instabilities was developed including the study of the mass and stiffness matrices of components. This model which identifies the stable and instable areas by an eigenvalue analysis is validated by modal analysis of components and by the instabilities tests.

This experimental and theoretical study brings us a better knowledge of the wiper system behavior and the instability phenomena. It also gives a general comprehension on the most influencing parameters on the occurrence of instabilities. Moreover, the experimental results allowed to validate the theoretical model. This existing model will define the design rules for new wiper systems. More precisely, it will provide us an engineer tool to improve the robustness of the system by sensitivity analysis. This study represents a rigorous and structured approach of the instability phenomena and will help us to anticipate the dynamic behavior of the system without any prototyping.

REFERENCES

1. Begout, M. "Les problèmes liés au frottement élastomère – verre dans l'automobile" Mémoire de thèse, université Paul Sabatier Toulouse, n°2206 (1979)

2. Grenouillat, R. "Etude des défauts d'essuyage : application à l'analyse prédictive" Mémoire de thèse, Ecole Centrale de Lyon (2001)

3. Muradore, F., Dreher, T., Jan, S. "Windshield Shape Optimization Using Neural Network" SAE Article, (2004)

4. Earles, S.W.E., Badi, M.N.M. "Oscillatory instabilities generated in a double pin-disc undamped system : a mechanism of disc-brake squeal" Proc. Instn. Mech. Engre, Vol 198 C, n°4, pp 43-50 (1984)

5. Moirot, F., Nguyen, Q.S., "Brake squeal : a problem of flutter instability of the steady sliding solution ? " Arch. Mech., 52, 4-5, pp 645-661 (2000)

6. Okura, S., Sekigushi, T. "Dynamic analysis of blade reversal behaviour in a windshield wiper system" SAE Papers, 2000-01-0127 (2000)

7. Codfert, V. "Modélisation globale d'un système d'essuyage" Mémoire de thèse, université des Sciences et Technologies de Lille (1997)

8. Koenen, A. "Rapport de synthèse sur le frottement du caoutchouc" Rapport n°03 98 186, Laboratoire de Tribologie VSE, La Verrière (1998)

9. J.F.Imbert "Analyse des structures par éléments finis" Cepadues Editions, ISBN 2.85.428.273.6 (1995)

10. Craig, R.R., Bampton M.C.C. "Coupling of substructures for dynamic analysis" American Institute of Aeronautics and Astronautics Journal, Vol. 6(7), pp. 1313-1319 (1968)

11. Chevennement-Roux, C., Grenouillat, R., Dreher, T., Alliot, P., Aubry, E., Laine, J.P., Jézéquel, L. "Mise en évidence des instabilités d'un système d'essuyage par analyse vibratoire-corrélation avec un modèle théorique" XIV^{e} Colloque Vibrations Chocs et Bruit, Ecole Centrale Lyon (2004)

12. Chambrette, P. "Stabilité des systèmes dynamiques avec frottement sec : application au crissement des freins à disque" Mémoire de thèse, Ecole Centrale Lyon, n°91-48 (1990)

13. Boudot, J.P. "Modélisation des bruits de freinage des véhicules industriels" Mémoire de thèse, Ecole Centrale Lyon, n°95-08 (1995)

14. J.J.Sinou "Synthèse non-linéaire des systèmes vibrants. Application aux systèmes de freinage" Mémoire de thèse, Ecole Centrale de Lyon (2002)

15. J.Guckenheimer and P.Holmes "Nonlinear Oscillations, Dynamical Systems, and Bifurcations of vector Fields" Springer-Verlag (1986)

16. A.H.Nayfeh and B.Balachandran "Applied Nonlinear Dynamics : Analytical, Computational and Experimental Methods" John Wiley & Sons (1995)